

A Low Hardware Complexity Time Domain Quantizer for Wideband Multibit $\Sigma\Delta$ ADCs

Pankaj Jha, Pravanjan Patra, *Student Member, IEEE*, Ashudeb Dutta, *Member, IEEE*
 Department of Electrical Engineering, Indian Institute of Technology Hyderabad, India-502205
 Email: jovialjha@gmail.com; pravanjanpatra80@gmail.com; asudeb_dutta@iith.ac.in

Abstract—This paper presents proof of concept of a low hardware complexity time domain quantizer (TDQ) for wideband multibit continuous time (CT) $\Sigma\Delta$ ADCs. Besides rendering multi-level quantization of the input signal, the proposed scheme generates a two-level loop feedback signal for the modulator. The two-level feedback eliminates the errors emanating from component mismatches in the feedback digital-to-analog converter (DAC) due to process variations. The complete scheme is modeled using Simulink (MATLAB) and is validated through simulation. A 2^{nd} order $\Sigma\Delta$ modulator incorporating the proposed TDQ achieves a dynamic range of 45.7 dB for a bandwidth of 10 MHz and an input sine-wave of -5.78 dBFS amplitude.

I. INTRODUCTION

Oversampling compounded with the noise-shaping capability, makes $\Sigma\Delta$ ADCs the most hankered choice in high-resolution applications [1]. These two characteristic features endow them with superior linearity, reduced anti-aliasing filtering requirements and straightforward analog implementation. Small feature size, low parasitic capacitances, lower power supply levels and high clock rates characterize contemporary and future VLSI technologies. Also, Pelgrom's mismatch model relates the local fluctuations of any device parameter under scaling to an area term, i.e., mismatch $\sim \frac{1}{\sqrt{WL}}$ [2] [3]. It implies that narrow devices show more mismatch and scaled VLSI technologies are more likely to be afflicted by poor component matching. In this regard a $\Sigma\Delta$ modulator, which offers greater immunity to circuit nonidealities and component mismatches, due to oversampling and their noise shaping behavior, becomes the most apt candidate for the implementation of high resolution (≥ 16 bits) ADCs in scaled VLSI technologies. The modulator has proved its superiority specially for applications where the motive is digitization of overall signal, or “*signal acquisition*”, rather than “*sample-by-sample data acquisition*” [4]. Moreover, $\Sigma\Delta$ ADCs offer more degrees of freedom for design (viz. order of the loop filter, oversampling ratio and the resolution of the internal quantizer) compared to other ADC architectures, hence easing the design procedure involving different trade-offs. Depending upon whether the sampling is done before or within the loop, $\Sigma\Delta$ modulators can be categorized into discrete-time (DT) and continuous-time modulators (CT). DT modulators sample the signal just before the modulator

loop and are implemented using switched capacitor circuits. For a continuous-time modulator, sampling is done just before the internal quantizer and is implemented using RC filters. The CT modulators have an edge over DT modulators in the following terms : (i) relaxed settling requirement for the integrators, making them more suitable for high frequency applications [6] (ii) the CT loop renders additional anti-aliasing for the input signal [5](iii) lower thermal-noise contribution of the integrator stages [6] (iv) avoids the use of switches, hence reducing the burden of implementing efficient switches in low-end technologies [7] (v) exhibit lower figure of merit (FOM) and are more area efficient [9].

Based on the resolution of the internal quantizer the $\Sigma\Delta$ modulators can be categorized into single bit (the internal quantizer is a comparator generally) and multibit (the internal quantizer is a multibit ADC e.g. flash, SAR, etc.) modulators. Single bit quantizers (only two levels of quantization) are inherently linear and exhibit insensitivity to process and component variations, achieve better figure of merit (FOM) and are more area efficient compared to their multibit counterparts [8][9]. Advantages of a multibit topology over the single bit counterparts are as follows: (i) increment in overall dynamic range (DR) by roughly 6dB per bit of the internal quantizer (ii) alleviates the effect of idle tone and noise pattern (iii) increased randomness of the quantization noise makes the analysis using white noise approximation more valid (iv) better stability, hence higher order NTFs can be utilized (v) works with a smaller OSR (for a target SNDR) leading to a lower complexity decimation filter, reduces power consumption of both the modulator and corresponding decimation filter, and hence apt for wideband applications [4] [10].

Taking cue from the above discussion, CT modulators have been employed to design efficient multibit wideband converters to bring together the individual advantages of the CT and multibit topologies [11]. However, multibit designs are limited by the strict accuracy requirements on the feedback DAC, emanating from the process and component mismatches. To explicate the effect of DAC errors on the output of the modulator, a linearized model of a $\Sigma\Delta$ modulator is shown in Fig. 1. The loop filters, $H_1(z)$ and $H_2(z)$ are defined as

$$H_1 = \frac{0.5 * z^{-1}}{(1 - z^{-1})}; \quad H_2 = \frac{2 * z^{-1}}{(1 - z^{-1})} \quad (1)$$

All the error/noise sources viz. $N_1(z), N_2(z), N_3(z)$ and $N_4(z)$, depending on the where they appear within the loop, are included as independent inputs, similar to the desired signal $P(z)$. The transfer function of the modulator's output, $Q(z)$, with respect to each of the mutually independent inputs are

$$STF(z) = \frac{Q(z)}{P(z)} = \frac{H_1 H_2}{1 + H_1 H_2 + H_2} = z^{-2} \quad (2)$$

$$NTF_1(z) = \frac{Q(z)}{N_1(z)} = \frac{H_1 H_2}{1 + H_1 H_2 + H_2} = z^{-2} \quad (3)$$

$$NTF_2(z) = \frac{Q(z)}{N_2(z)} = \frac{H_2}{1 + H_1 H_2 + H_2} = 2z^{-1}(1 - z^{-1}) \quad (4)$$

$$NTF_3(z) = \frac{Q(z)}{N_3(z)} = \frac{1}{1 + H_1 H_2 + H_2} = (1 - z^{-1})^2 \quad (5)$$

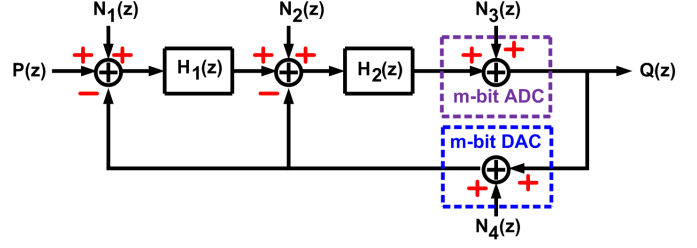
$$NTF_4(z) = \frac{Q(z)}{N_4(z)} = -\frac{H_1 H_2 + H_2}{1 + H_1 H_2 + H_2} = -z^{-1}(2 - z^{-1}) \quad (6)$$

where, STF is the signal transfer function and NTFs are the noise transfer functions. Magnitude plots for all the NTFs are shown in Fig. 1. The plots clearly show that noise-shaping increases from $NTF_1(z)$ to $NTF_2(z)$ to $NTF_3(z)$, which implies that the in-band power of a source of error in the forward path of the loop will decrease with an increase in the proximity of the source and quantizer. Moreover, since the error in the feedback path $NTF_4(z)$ is added directly to the input, it passes on to the output of the modulator without any shaping. The error due to component mismatch in the DAC corresponds to $NTF_4(z)$ here. Therefore the overall accuracy of the modulator is no better than that of the feedback DAC. Also, assuming a Gaussian distribution for variation of the actual value of each unit element (capacitors, resistors, current sources, etc.), the worst-case relative error in a B -bit DAC output can be estimated as

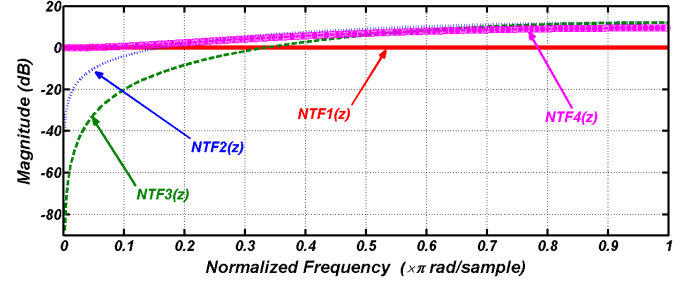
$$\sigma \left\{ \frac{\Delta y}{y} \right\} = \frac{1}{2 * \sqrt{2^B}} * \sigma \left\{ \frac{\Delta U_e}{U_e} \right\} \quad (7)$$

where, $\frac{\Delta U_e}{U_e}$ is the relative error in the unit element used to reconstruct the analog feedback signal [12][19].

A typical lithographical renders a component matching of 0.1-0.5% (\sim 8-10 bit resolution) [14]. To achieve a higher resolution, Flash ADC, if used as the internal quantizer in the modulator, necessitates trimming of the intermediate reference levels [15]. But trimming requires additional circuitry. Also the comparators require additional offset correction [16]. [17] replaces flash ADC with SAR ADC as the internal quantizer of the modulator. Important techniques to correct the DAC error are as follows : (i) external trimming [18] [19] (ii) utilizing two different DACs, one single bit and other multibit [20] (iii) multibit quantization



(a) Linearized model of a 2^{nd} order $\Sigma\Delta$ modulator.



(b) Magnitude plots for all NTFs.

Fig. 1. A simple model of a $\Sigma\Delta$ modulator to understand the effect of relevant noise sources on the modulator's output.

but single bit feedback [21] (iv) digital error correction [14][4][22][23][24] (v) various data element matching techniques (DEM), like randomization algorithms [25], clocked averaging [26], individual level averaging (ILA) [27], data weighted averaging (DWA) [28], data directed scrambling (DDS) [29], vector-quantizer structures [30]. Lately to circumvent the problem of DAC non-linearity, there has been an inclination to shifting the voltage-domain signal processing to time-domain processing. This scheme exploits the usage of arbiters (i.e., flip-flops) in place of comparators making it suitable for advanced CMOS technologies with low supply voltage and fast switching speed[31]. Numerous works involving time-domain signal processing employ voltage-controlled oscillators and gated-ring oscillators [31][32][33][34][35][36][37][38]. A time encoding quantizer was presented in [39][40][41][42][43]. Modulators with time-domain quantizers (TDQ) utilizing pulse wave modulation (PWM) and pulse position modulation (PPM) have been introduced in [44][45][46][47].

In this paper, a 2^{nd} order $\Sigma\Delta$ modulator with a new TDQ is demonstrated. The scheme utilizes a pulse wave modulator to convert the voltage-domain information to time-domain by modulating the width of the pulse proportional to the input voltage. This time-domain information, or width of the pulse, is then quantized in terms smaller time steps using a counter. The signal which needs to be fed back to the loop is also derived from the output of the counter. The obtained feedback is fit for 1-bit DAC, eliminating the problem of feedback DAC linearity. It is better scheme than [44] in terms of utilizing lesser hardware, and hence is more area efficient.

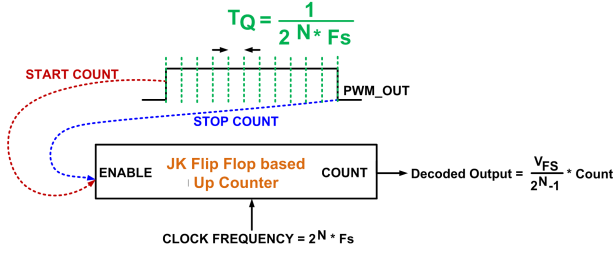


Fig. 2. Basic scheme of the proposed TDQ.

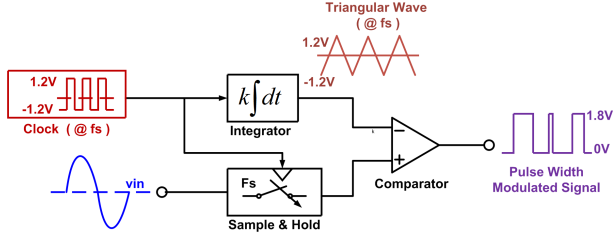


Fig. 3. Block diagram of the PWM generator.

The organization of this paper is as follows. Section II introduces the proposed TDQ and mentions the design parameters used for modeling the TDQ and $\Sigma\Delta$ modulator. The experimental results and conclusions are given in Section III and Section IV, respectively.

II. MODIFIED TIME-DOMAIN QUANTIZER

Fig. 2 illustrates the basic scheme of the proposed time domain quantizer. The PWM generator outputs pulses, PWM_OUT , whose widths are proportional to the input voltage. The PWM_OUT signal acts as the *enable* signal for a counter, working as a time to digital converter (TDC). The counter operating at a high frequency (multiples of the sampling frequency of the modulator) counts the number of time steps, T_Q , within the width of the pulse generated by the PWM. A N -bit voltage-domain quantizer divides the full scale voltage range into 2^N levels. Emulating the same concept, the N -bit TDC requires a N -bit counter so that the pulse with maximum width can be divided into 2^N time steps T_Q . Therefore, the counter needs to be operating at a frequency of $2^N * F_S$, where F_S is the sampling frequency of the modulator. The feedback signal is derived by *ORing* the outputs ($Q_0 - Q_5$) of the counter and it emulates the 1-bit feedback signal in the case of single bit modulators. Hence this scheme does away with the stringent requirements of DAC accuracy in multibit topology.

A. PWM Generator

The block diagram of the PWM generator is depicted in Fig. 3. A clock pulse signal of frequency of F_S , where F_S is the sampling frequency of the modulator, is integrated to obtain a triangular wave with same frequency. This triangular wave along with the input sampled at F_S are fed to a comparator. The comparator outputs a PWM signal whose pulse

width is proportional to the input voltage. Hence, the voltage-domain information is encapsulated into width of the pulse in time-domain. It is worth mentioning here that compared to that in [44], double sampling is not required in the proposed scheme. Thus a single comparator is enough vis-a-vis two comparators necessary in [44]. Also the proposed scheme samples the input at a rate half that of [44], so the proposed scheme is comparatively less effected by errors emanating from clock jitter.

The simulation parameters used for the PWM generator for the proposed TDQ are given in Table I.

TABLE I
SIMULATION PARAMETERS FOR PWM GENERATOR

Parameter	Value
Modulator sampling frequency	250MHz
Input signal sampling frequency	250MHz
Clock frequency	250MHz
Triangular wave frequency	250MHz
Triangular wave peak-to-peak voltage range	$\pm 1.2V$

B. TDC with loop feedback signal generation

The PWM_OUT signal acts as an enable signal for the TDC. The TDC consists of a JK flip flop based up-counter. The counter essentially counts the number of smaller time steps, T_Q , hence emulating a conventional quantizer with its quantization error (see Fig. 2). In order to obtain N -bit resolution the counter is operated at a frequency of $2^N * F_S$, where F_S is the sampling frequency of the modulator. At the same time it is noticeable that only $M = \log_2(N)$ flip-flops is enough to achieve the same resolution. The counter starts to count at positive edge of the PWM_OUT and is reset at its negative edge. The count corresponding to each pulse is also latched at same negative edge. A normal JK flip-flop in the Simulink (MATLAB) library is modified to include the reset functionality as shown in Fig. 4. A synchronous up-counter is built using the modified JK flip-flop as shown Fig. 5.

Finally taking clue from the fact a 1-bit $\Sigma\Delta$ ADC outputs more number of logic ones for a higher input amplitude, it is contemplated that the loop feedback signal needs to be held at logic high for a period proportional to the input signal amplitude. Hence the feedback signal is generated by *ORing* each of the M bits of the counter.

The simulation parameters used for the TDC for the proposed TDQ are given in Table II.

TABLE II
SIMULATION PARAMETERS FOR TDC

Parameter	Value
Desired quantizer resolution	6 bits
Counter operating frequency	$(2^6 * 250MHz =)16GHz$
Number of flip-flops used	6

The complete TDQ is shown in Fig. 6.

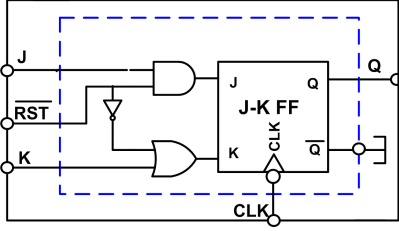


Fig. 4. JK flip-flop from the Simulink library modified to include reset facility.

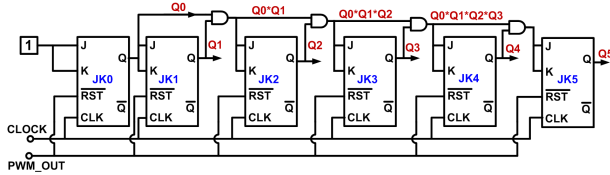


Fig. 5. Block diagram of the up-counter implemented using the modified JK flip-flop shown in the previous figure.

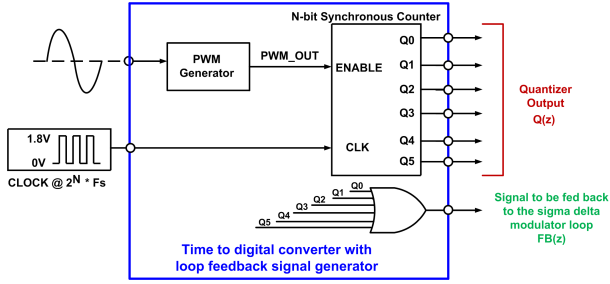


Fig. 6. Block diagram of the proposed TDQ.

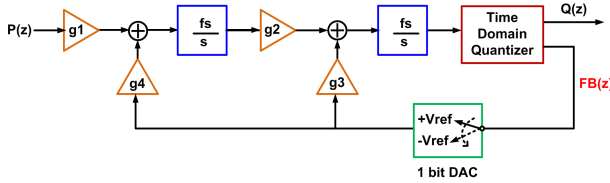


Fig. 7. Block diagram of the 2^{nd} order CT $\Sigma\Delta$ modulator loop incorporating the proposed TDQ.

C. Continuous-time $\Sigma\Delta$ modulator incorporating the proposed TDQ

The 2^{nd} order CT $\Sigma\Delta$ modulator loop incorporating the proposed TDQ is shown in Fig. 6. Here the coefficients, g_1, g_2, g_3 and g_4 , are fixed (using the concept of dynamic loop scaling) such that the output of the second integrator does not exceed the peak-to-peak voltage range of the triangular wave obtained from the PWM generator (see Fig. 3). The loop coefficients and simulation parameters are given in Table III.

III. SIMULATION RESULTS

To validate the proposal the complete scheme described above is modeled using Simulink (Matlab). The Fig. 8 shows the output of each of the integrator in the modulator, and the

TABLE III
SIMULATION PARAMETERS FOR $\Sigma\Delta$ MODULATOR

Parameter	Value
g_1	0.2
g_2	0.7
g_3	0.6
g_4	0.3
F_S	250MHz
V_{REF}	1.225V
Input amplitude	-5.78dB
Input frequency	1 MHz

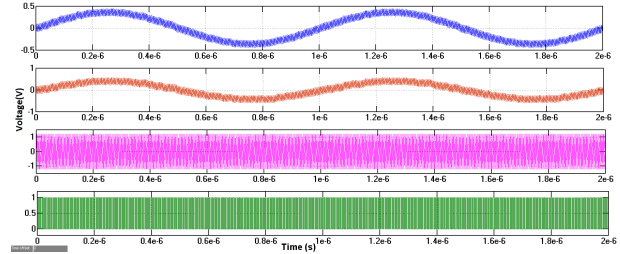


Fig. 8. Output waveform of each of the integrator in the modulator, and the PWM generator. The plots are arranged as - output of first integrator, output of the second integrator, triangular wave and PWM wave (in sequence from top to bottom).

PWM generator. As is clear from the figure, the peak-to-peak output of the second integrator never exceeds the peak-to-peak voltage range of the triangular wave. The outputs of the TDC along with the feedback signal for the loop for one of the pulses generated by the PWM generator is shown in Fig. 9. It is evident from the figure that counter starts to count at arrival of the first clock pulse after positive edge of the PWM_OUT and is reset at its negative edge. Also the feedback signal, hence generated, closely matches the input pulse with some quantization error. The power spectral density of the output of the $\Sigma\Delta$ modulator, described in the previous section, is shown in Fig. 10. The $\Sigma\Delta$ modulator achieves 45.7dB signal to noise distortion ratio (SNDR) for a input sine-wave of 1MHz frequency and -5.78dB amplitude. Therefore, the proposed scheme for a TDQ works as desired and is compatible with a $\Sigma\Delta$ modulator. More importantly, it is worth noticing that the proposed quantizer renders the same functionality of [44], but with a significantly lower hardware requirement. The proposed PWM generator requires only one comparator vis-a-vis two comparators necessary in [44]). Additionally, the proposed N -bit TDC uses only N flip-flops compared to 2^N used in [44].

IV. CONCLUSION

$\Sigma\Delta$ modulator with a new scheme for TDQ has been proposed. All the required modules have been modeled using Simulink (MATLAB) library blocks and the proposed scheme is validated through simulations. The proposed TDQ works as desired, and more importantly, with considerably lesser hardware requirements. This system is intended for wideband applications.

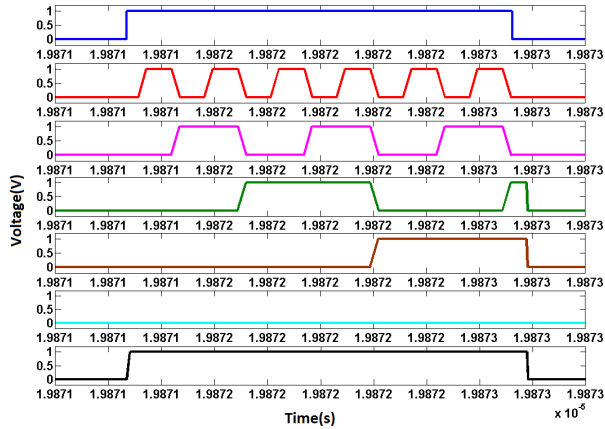


Fig. 9. The output of the TDC along with the feedback signal for the loop for a specimen pulse generated by the PWM generator is shown in Fig. 9. The outputs are arranged as - the pulse from PWM generator, Q_0 (LSB), Q_1 , Q_2 , Q_3 , Q_4 , Q_5 (MSB) and the feedback signal (in sequence from top to bottom).

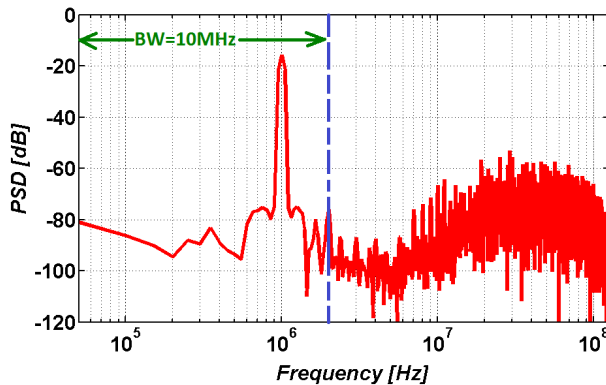


Fig. 10. The power spectral density of the output of the $\Sigma\Delta$ modulator shown in Fig.7 .

TABLE IV
PERFORMANCE OF $\Sigma\Delta$ ADC WITH TDQ

Parameter	Value	
	This work	[44]
Order	2^{nd}	3^{rd}
Bandwidth (MHz)	10	20k
F_s (MHz)	250	250
V_{REF} (V)	1.225	1.2
Input amplitude (dB)	-5.78	-5
SNDR (dB)	45.7	60

REFERENCES

- [1] Boser, B.E.; Wooley, B.A., "The design of sigma-delta modulation analog-to-digital converters," IEEE Journal of Solid-State Circuits, , vol.23, no.6, pp.1298-1308, Dec 1988.
- [2] Pelgrom, M.J.M.; Tuinhout, H.P.; Vertregt, M., "Transistor matching in analog CMOS applications," International Electron Devices Meeting, 1998. IEDM '98. Technical Digest., vol., no., pp.915,918, 6-9 Dec. 1998.
- [3] Lovett, S.J.; Welten, M.; Mathewson, A.; Mason, B., "Optimizing MOS transistor mismatch," IEEE Journal of Solid-State Circuits, vol.33, no.1, pp.147,150, Jan 1998.
- [4] Sarhang-Nejad, M.; Temes, G.C., "A high-resolution multibit ADC with digital correction and relaxed amplifier requirements," IEEE Journal of Solid-State Circuits, vol.28, no.6, pp.648,660, Jun 1993.
- [5] Schreier, R.; Zhang, B., "Delta-sigma modulators employing continuous-time circuitry," IEEE Transactions on Circuits and Systems I: Fundamental Theory and Applications., vol.43, no.4, pp.324,332, Apr 1996.
- [6] Continuous-Time Delta-Sigma Modulators for High-Speed A/D Conversion: Theory, Practice and Fundamental Performance Limits J. A. Cherry and W. M. Snelgrove, 2002, Kluwer.
- [7] Dhanasekaran, V.; Gambhir, M.; Elsayed, M.M.; Sanchez-Sinencio, E.; Silva-Martinez, J.; Mishra, C.; Lei Chen; Pankratz, E.J., "A Continuous Time Multi-Bit ADC Using Time Domain Quantizer and Feedback Element," Solid-State Circuits, IEEE Journal of , vol.46, no.3, pp.639,650, March 2011.
- [8] Agrawal, B.; Sheno, K., "Design Methodology for $\Sigma\Delta$," Communications, IEEE Transactions on , vol.31, no.3, pp.360,370, Mar 1983.
- [9] Yann Le Guillou; "Analyzing sigma-delta ADCs in deep-submicron CMOS technologies," Philips Semi-conductors Innovation Centre for RF technologies, 2005.
- [10] CMOS Cascade Sigma-Delta Modulators for Sensors and Telecom : Error Analysis and Practical Design, R. del Rio, F. Medeiro, B. Prez-Verd, J.M. de la Rosa, . Rodriguez-Vzquez, ISBN-13 978-1-4020-4776-2.
- [11] G. Mitteregger, C. Ebner, S. Mechnig, T. Blon, C. Holuigue, E. Romani, A. Melodia and V. Melini, "A 14 b 20 mW 640 MHz CMOS CT $\Sigma\Delta$ ADC with 20 MHz signal bandwidth and 12 b ENOB", IEEE ISSCC Dig. Tech. Papers, pp. 131-140, 2006.
- [12] B. Razavi, Principles of Data Converter System Design. IEEE Press, 1995.
- [13] L.R. Carley, R. Schreier, and G.C. Temes, Delta-Sigma ADCs with Multibit Internal Converters, Chapter 8 in Delta-Sigma Data Converters: Theory, Design and Simulation (S.R. Norsworthy, R. Schreier, and G.C. Temes, Editors). IEEE Press, 1997.
- [14] Thompson, C.D.; Bernadas, S.R., "A digitally-corrected 20b delta-sigma modulator," IEEE International Solid-State Circuits Conference, 1994. Digest of Technical Papers. 41st ISSCC., 1994 , vol., no., pp.194,195, 16-18 Feb. 1994.
- [15] de la Rosa, J.M., "Sigma-Delta Modulators: Tutorial Overview, Design Guide, and State-of-the-Art Survey," IEEE Transactions on Circuits and Systems I: Regular Papers, vol.58, no.1, pp.1,21, Jan. 2011.
- [16] Mitteregger, G.; Ebner, C.; Mechnig, S.; Blon, T.; Holuigue, C.; Romani, E., "A 20-mW 640-MHz CMOS Continuous-Time $\Sigma\Delta$ ADC With 20-MHz Signal Bandwidth, 80-dB Dynamic Range and 12-bit ENOB," IEEE Journal of Solid-State Circuits, vol.41, no.12, pp.2641,2649, Dec. 2006.
- [17] Samid, L.; Abu-ghazi, M.; Manoli, Y., "A novel continuous-time $\Sigma\Delta$ modulator with a successive approximation multibit quantizer," Circuits and Systems, 2003 IEEE 46th Midwest Symposium on , vol.1, no., pp.59,63 Vol. 1, 30-30 Dec. 2003.
- [18] R. W. Adams, Design and implementation of an audio 18-bit analog-to-digital converter using oversampling techniques, J. Audio Eng., vol. 34, no. 3, pp. 153-166, Mar. 1986.
- [19] L.R. Carley, R. Schreier, and G.C. Temes, Delta-Sigma ADCs with Multibit Internal Converters, Chapter 8 in Delta-Sigma Data Converters: Theory, Design and Simulation (S.R. Norsworthy, R. Schreier, and G.C. Temes, Editors). IEEE Press, 1997.
- [20] Brandt, B.P.; Wooley, B.A., "A 50-MHz multibit sigma-delta modulator for 12-b 2-MHz A/D conversion," Solid-State Circuits, IEEE Journal of , vol.26, no.12, pp.1746,1756, Dec 1991.
- [21] Leslie, T.C.; Singh, B., "An improved sigma-delta modulator architecture," Circuits and Systems, 1990., IEEE International Symposium on , vol., no., pp.372,375 vol.1, 1-3 May 1990.
- [22] Cataltepe, T.; Kramer, A.R.; Larson, L.E.; Temes, G.C.; Walden, R.H., "Digitally corrected multi-bit data converters," Circuits and Systems, 1989., IEEE International Symposium on , vol., no., pp.647,650 vol.1, 8-11 May 1989.
- [23] Larson, L.E.; Cataltepe, T.; Temes, G.C., "Multibit oversampled - A/D converter with digital error correction," Electronics Letters , vol.24, no.16, pp.1051,1052, 4 Aug 1988.
- [24] R.H. Walden, T. Cataltepe, and G.C. Temes, Architectures for higher-order multi-bit $\Sigma\Delta$ modulators. Proc. of the IEEE International Symposium Circuits and Systems, vol. 5, pp. 895-898, 1990.

- [25] L.R. Carley and J. Kenney, A 16-bit 4th order noise-shaping D/A converter. Proc. of the IEEE Custom Integrated Circuits Conference, pp. 21.7.1-4, 1988.
- [26] K.B. Klaasen, Digitally controlled absolute voltage division. IEEE Transactions on Instrumentation and Measurement, vol. 24, no. 3, pp. 106-112, June 1975.
- [27] B. Leung and S. Sutarja, Multibit $\Sigma\Delta$ A/D Converter Incorporating a Novel Class of Dynamic Element Matching Techniques. IEEE Transactions on Circuits and Systems - II, vol. 39, pp. 35-51, January 1992.
- [28] R.T. Baird and T. Fiez, Linearity Enhancement of Multibit $\Sigma\Delta$ A/D and D/A Converters using Data Weighted Averaging. IEEE Transactions on Circuits and Systems - II, vol. 42, pp. 753-762, December 1995.
- [29] R.W. Adams and T.W. Kwan, Data-directed scrambler for multi-bit noise-shaping D/A converters. U.S. Patent 5,404,142, 1995.
- [30] R. Schreier and B. Zhang, Noise-shaped multibit D/A converter employing unit elements. Electronics Letters, vol. 31, pp. 1712-1713, September 1995.
- [31] Yu, W.; Kim, J.; Kim, K.; Cho, S., "A Time-Domain High-Order MASH $\Delta\Sigma$ ADC Using Voltage-Controlled Gated-Ring Oscillator," Circuits and Systems I: Regular Papers, IEEE Transactions on , vol.60, no.4, pp.856,866, April 2013.
- [32] J. Kim and S. H. Cho "A time-based analog-to-digital converter using a multi-phase voltage-controlled oscillator" Proc. IEEE Int. Symp. Circuits Syst., pp. 3934-3937, 2006.
- [33] Y. Yoon , J. Kim , T. Jang and S. H. Cho "A time-based bandpass ADC using time-interleaved voltage-controlled oscillators" IEEE Trans. Circuits Syst. I, Reg. Papers, vol. 55, pp. 3571-3581, 2008.
- [34] J. Kim , T. Jang , Y. Yoon and S. H. Cho "Analysis and design of voltage-controlled oscillator based analog-to-Digital converter" IEEE Trans. Circuits Syst. I, Reg. Papers, vol. 57, pp. 18-30, 2010.
- [35] J. Daniels , W. Dehaene , M. Steyaert and A. Wiesbauer "A 0.02 mm² 65 nm CMOS 30 MHz BW all-digital differential VCO-based ADC with 64 dB SNDR" Proc. IEEE Symp. VLSI Circuits Dig. Tech. Papers, pp. 155-156, 2010.
- [36] G. Taylor and I. Galton "A mostly-digital variable-rate continuous-time Delta-Sigma modulator ADC" IEEE J. Solid-State Circuits, vol. 45, no. 12, pp. 2634-2646, 2010.
- [37] Y. Cao "A 1.7 mW 11 b 1-1-1 MASH $\Delta\Sigma$ time-to-Digital converter" Proc. IEEE Int. Solid-State Circuits Conf. Dig. Tech. Papers, pp. 480-482, 2011.
- [38] T. Konishi "A 40-nm 640 μm^2 45-dB opampless all-digital second-order MASH $\Delta\Sigma$ ADC" Proc. IEEE Int. Symp. Circuits Syst., pp. 518-521, 2011.
- [39] E. Prefasi, et al., A 0.1 mm² Wide Bandwidth Continuous-Time ADC Based on a Time Encoding Quantizer in 0.13 μm CMOS, IEEE J. Solid-State Circuits, vol. 44, no. 10, pp. 2745-2754, Oct. 2009.
- [40] Hernandez, L.; Prefasi, E., "Analog-to-Digital Conversion Using Noise Shaping and Time Encoding," IEEE Transactions on Circuits and Systems I: Regular Papers, IEEE Transactions on , vol.55, no.7, pp.2026,2037, Aug. 2008.
- [41] Corporales, L.H.; Prefasi, E.; Pun, E.; Paton, S., "A 1.2-MHz 10-bit Continuous-Time SigmaDelta ADC Using a Time Encoding Quantizer," Circuits and Systems II: Express Briefs, IEEE Transactions on , vol.56, no.1, pp.16,20, Jan. 2009.
- [42] Prefasi, E.; Paton, S.; Hernandez, L., "A 7 mW 20 MHz BW Time-Encoding Oversampling Converter Implemented in a 0.08 mm² 65 nm CMOS Circuit," IEEE Journal of Solid-State Circuits, vol.46, no.7, pp.1562,1574, July 2011.
- [43] Prefasi, E.; Paton, S.; Hernandez, L.; Gaggl, R.; Wiesbauer, A.; Hauptmann, J., "A 0.08 mm², 7mW Time-Encoding Oversampling Converter with 10 bits and 20MHz BW in 65nm CMOS," ESSCIRC, 2010 Proceedings of the , vol., no., pp.430,433, 14-16 Sept. 2010.
- [44] Dhanasekaran, V.; Gambhir, M.; Elsayed, M.M.; Sanchez-Sinencio, E.; Silva-Martinez, J.; Mishra, C.; Lei Chen; Pankratz, E.J., "A Continuous Time Multi-Bit $\Delta\Sigma$ ADC Using Time Domain Quantizer and Feedback Element," IEEE Journal of Solid-State Circuits, vol.46, no.3, pp.639,650, March 2011.
- [45] Wooyoung Jung; Mortazavi, Y.; Evans, B.L.; Hassibi, A., "An all-digital PWM-based ADC with an inherently matched multi-bit quantizer," IEEE Proceedings of the Custom Integrated Circuits Conference (CICC), 2014, vol., no., pp.1,4, 15-17 Sept. 2014.
- [46] Chongjun Ding; Manoli, Y.; Keller, M., "A time-domain based multi-bit ADC for application in Delta-Sigma modulators," IEEE International Symposium on Circuits and Systems (ISCAS), 2014 , vol., no., pp.930,933, 1-5 June 2014.
- [47] Naraghi, S.; Courcy, M.; Flynn, M.P., "A 9-bit, 14 W and 0.06 mm Pulse Position Modulation ADC in 90 nm Digital CMOS," IEEE Journal of Solid-State Circuits, IEEE Journal of , vol.45, no.9, pp.1870,1880, Sept. 2010.
- [48] Naraghi, S.; Courcy, M.; Flynn, M.P., "A 9-bit, 14 W and 0.06 mm Pulse Position Modulation ADC in 90 nm Digital CMOS," IEEE Journal of Solid-State Circuits, IEEE Journal of , vol.45, no.9, pp.1870,1880, Sept. 2010.
- [49] Naraghi, S.; Courcy, M.; Flynn, M.P., "A 9-bit, 14 W and 0.06 mm Pulse Position Modulation ADC in 90 nm Digital CMOS," IEEE Journal of Solid-State Circuits, IEEE Journal of , vol.45, no.9, pp.1870,1880, Sept. 2010.